ASME Open Journal of Engineering
Online journal at:
https://asmedigitalcollection.asme.org/openengineering

Multi-Objective Optimization and Tradespace Analysis of a Mechanical Clock Movement Design

Yifan Xu
Department of Mechanical Engineering,
Clemson University,
261 Fluor Daniel EIB,
Clemson, SC 29634
e-mail: yxu5@clemson.edu

Cameron Turner
ASME Membership #4464322
Department of Mechanical Engineering,
Clemson University,
261 Fluor Daniel EIB,
Clemson, SC 29634
e-mail: cturne9@clemson.edu

John Wagner[1]
ASME Membership #1280510
Department of Mechanical Engineering,
Clemson University,
261 Fluor Daniel EIB,
Clemson, SC 29634
e-mail: jwagner@clemson.edu

Pendulum clocks were the prevalent time keeping standard for centuries to regulate commerce and public activities. These mechanical movements were the most accurate timekeepers globally until replaced by electric clocks. Although mainly used for decorative purposes today, the pendulum clock's working principles and mechanical behavior can serve to demonstrate fundamental science and engineering concepts. The tradeoff between a clock's quality factor, pendulum properties, and period can best be explored with multiple objective optimization and tradespace analysis methods. In this project, a Multi-Objective Genetic Algorithm (MOGA-II) and a Multi-Objective Simulated Annealing (MOSA) optimization approaches are applied to evaluate a Graham escapement street clock for pendulum mass and time accuracy with a range of the period. These clock designs vary the pendulum length, pendulum bob radius, and bob thickness. Horological concepts are used to calculate the overall performance and general utility. The numerical results show a 0.7% increase in the quality factor, and a 0.56% reduction in the mass, while maintaining the designed period by modifying the clock parameters. More importantly, these changes can provide material cost savings in a mass production scenario. Overall, the study highlights the tradeoff designer engineers have considered for decades which can now be visualized using computer tools for greater insight. [DOI: 10.1115/1.4062410]

Keywords: design, design engineering, design methodology, design optimization, experimental, mechanical engineering simulation, modeling, optimization

1 Introduction

A mechanical clock as shown in Fig. 1 converts potential energy into impulsed oscillating pendulum or balance wheel motion that can be harnessed to display the passage of time. The typical clock uses a hanging weight or coiled spring as the power source to drive the gear train, dial hands, escapement, and pendulum [1]. The escapement engages symmetrically with a multi-toothed escape wheel through dual pallets and a crutch to discretize rotational motion into pendulum swing [2]. In this manner, the pendulum, usually a round or cylindrical weight on a wooden rod, maintains periodic oscillations. The pendulum's period primarily depends on the rod length with a nominal small-angle of swing. A thin steel suspension spring vertically holds the pendulum while the crutch provides impulsive forces to the rod based on the escapement dynamics. The time display (minutes, hours) is driven by the gear train with a 12:1 motion work ratio for the hours. The innovative design of pendulum clocks served as the global time keeping standard until they were replaced by electric clocks [3]. The assorted components within the movement provide a platform to explore design tradeoffs and evaluation of the original factory product using optimization and tradespace analysis methods [4].

The design of a clock movement requires the consideration of various factors including overall size, material selection, timekeeping accuracy, and escapement type. Further, these factors may be influenced by each other. In this study, three fundamental characteristics will be explored—timekeeping accuracy, pendulum mass, and clock period deviation from the reference setpoint. The pendulum clock's accuracy is proportional to its quality factor, Q, as shown in Fig. 2 (The figure was modified from Ref. [5]). A detailed description of mechanical system quality factor has been provided by Smith [6]. The quality factor is a dimensionless parameter defined as the ratio of the energy stored to the energy lost in one period [7] [8]. In an oscillator system, the energy loss is proportional to the amplitude decrease. Thus, the quality factor can be obtained experimentally by measuring the time it takes for the amplitude decrease to $1/e$ of its original value.

Therefore, designers may want to maximize Q for better accuracy, which generally corresponds to less system resistance. The pendulum's mass is another essential factor that must be considered in the design phase. In most cases, a small, lightweight pendulum clock is desired by manufacturers as it consumes fewer materials and is easier to ship; however, the energy stored is a function of mass. The period difference from the ideal value contributes to

[1]Corresponding author.

Manuscript received December 1, 2022; final manuscript received April 17, 2023; published online May 12, 2023. Assoc. Editor: John Allen.

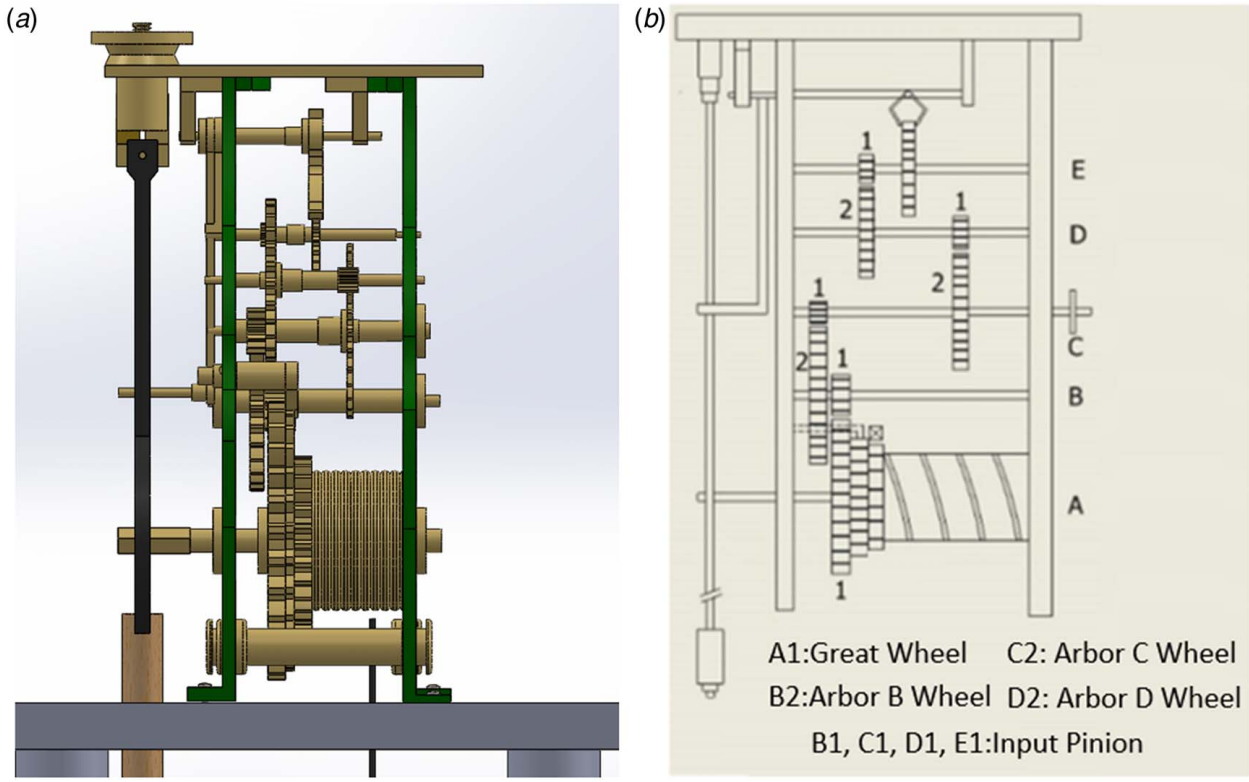

Fig. 1 Howard clock movement—(*a*) Three-dimensional CAD model for virtual engineering design studies, and (*b*) mechanism configuration with labels

established the daily accuracy. For the target street clock, a 2.0-second period is desired. These three characteristics are directly related to the geometry of the pendulum clock, and tradeoffs exist amongst them. Therefore, a method of determining the best design with optimal overall performance is necessary.

To evaluate these different design criteria, a Multiple Objective Optimization (MOO) method and Tradespace analysis will be applied. In general, engineering problems have conflicting objectives. Specifically, optimizing one objective often results in unacceptable results concerning the others [9]. Therefore, MOO methods are essential to determine solutions that satisfy all objectives at an acceptable level; such solutions are called optimal solutions [10]. Although single objective optimization offers a unique optimal solution, MOO may provide multiple optimal (Pareto) solutions. Pareto solutions are characterized in that an improvement in one objective will adversely impact at least one of the other objectives. MOO seeks to find the best Pareto solution. One approach is to begin by identifying all of the Pareto solutions and then selecting between them. However, full enumeration of the tradespace of Pareto solutions is usually computationally expensive at best and prohibitive in many cases. Thus, choosing an algorithm to find a subset of desirable Pareto solutions that represent the whole set is vital for MOO [11]. In this project, Multi-Objective Genetic Algorithm (MOGA-II) and Multi-Objective Simulated Annealing (MOSA) MOO algorithm are utilized. By comparing these results with a random solution approach, the MOO method's effectiveness may be explored in finding optimal solutions. Finally, a tradespace analysis method was applied by determining the highest utility design with a fixed cost to visually investigate the design space.

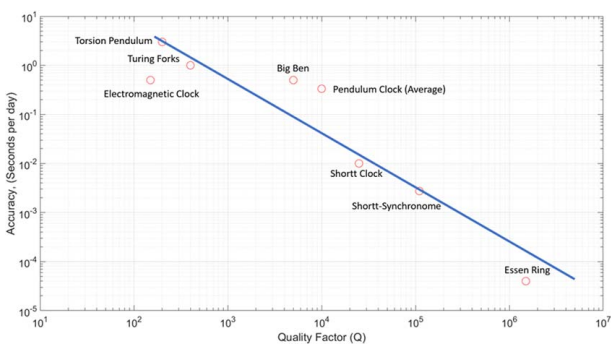

Fig. 2 Accuracy versus quality factor for mechanical clocks and oscillators

The optimal design of a pendulum clock with a MOO algorithm and tradespace analysis method will be investigated using a model-based approach with experimental validation. Representations of the tradespace are fundamentally based upon models that serve as representations of the potential design solutions [12–16]. In early stage design, tradespace analysis is often based on crude models that only represent the most fundamental behaviors of the design solutions [14,17]. The reason for this is obvious, at this stage of the design process, the system has generally not yet been designed. Yet, critical decisions need to be made concerning the direction and feasibility of the design project based on limited conceptual models of the design solution. Effective early stage models are known to be a critical element for tradespace tradeoff analysis [14–16,18–20] and often considerable effort is invested in the development of these models [15,16]. Unfortunately, many of these models do not fully represent the complete physics of the eventual system, particularly in the case of complex system design [12,15–17,19,21]. Nonetheless, the importance of the underlying models used to identify trade-off relations should not be underestimated.

The remainder of the paper is organized as follows: Sec. 2 introduces the fundamentals of MOO and two algorithms. Tradespace analysis methods will be presented in Sec. 3. In Sec. 4, the mathematical model for a pendulum clock, including escapement, is developed with experimental validation on a street clock. Representative numerical results are discussed to explore the various designs.

The summary is contained in Sec. 5. Finally, a complete Nomenclature List is provided.

2 Multiple Objective Optimization (MOO)

Engineering design problems often require the simultaneous optimization of multiple, often conflicting, objectives. A MOO problem can be solved by identifying the design variables, x_i, which are assembled into the design vector, $\bar{x} = (x_1, x_2, \ldots, x_n)$, to minimize the multiple objective functions $f_i(\bar{x})$ given as [22]

$$\min \quad \sum_{i=1}^{L} w_i f_i(\bar{x}) \tag{1a}$$

which are subject to the constraints:

$$g_j(\bar{x}) \leq 0 \quad \forall j \in J \tag{1b}$$

$$h_k(\bar{x}) = 0 \quad \forall k \in K \tag{1c}$$

$$\overline{x_L} \leq \bar{x} \leq \overline{x_H} \tag{1d}$$

The individual objective functions usually do not have their minimum value at the same set of design variables. Thus, the trade-off may need to consider conflicting objectives. A general approach to MOO problems is a Pareto solution, $\bar{x}_p(x_{p1}, x_{p2}, \ldots, x_{pn})$, such that no other solution can dominate it, i.e., a solution does not exist in which the objective functions' values are smaller than $f_i(\bar{x}_p)$. All the Pareto solutions form a set called the Pareto Frontier. Therefore, the goal is to identify a set of solutions that are as close as possible to, and uniformly distributed over the true Pareto frontier [22].

2.1 Genetic Algorithms (GA). Genetic algorithms (GA) are popular in finding Pareto solutions for MOO by encoding potential solutions using a "chromosome-like" data structure [23]. The process of natural selection has inspired the GA codes. In natural selection theory, a specie that carries genes fitting the environment has a higher chance of surviving and passing its genes to offspring. Therefore, their genes become increasingly dominant within their population. In some cases, random mutations occur and may change a portion of an individual's genes. If such mutations help individuals survive in the environment, then the new genes will be inherited by further generations. Otherwise, the mutated individual will be eliminated by the natural selection process. GA emulate this process, so each design variable set is called an "individual", and a collection of individuals is called a "population". Individuals consist of genes that are represented by binary strings. An encoding process is required to convert the design variables into such binary strings [11].

Pareto solutions may be achieved by repeating the "crossover" and "mutation" scenario for each iteration in the GA. In the crossover, two individuals (i.e., parents) who were selected based on the fitness of the population are combined to form a new individual (i.e., offspring). The crossover process may randomly select one or more crossover points to cut the genetic sequence into several pieces and swipe them afterward to recombine the sequence for the children. An offspring is expected to inherit the advantages of both of its parents and, therefore, has better fitness. The population will eventually converge by repeating this process, which means a single design variable set dominates it. However, in genetic algorithm, diverse or dissimilar optimal solution is desired. To achieve this goal a mutation step must be included to make Pareto solutions uniformly distributed over the Pareto frontier, including the ends. Mutation occurs at the gene level and alters one bit in the genetic sequence from its original state. Thus, new individuals were created that differ from the population.

The MOGA-II algorithm, based on the GA principle, was selected to solve the MOO problem. The process of MOGA-II may is shown in Fig. 3. Although the MOGA-II approach is similar for each GA stage, it uses a directional crossover along with selection crossover and mutation as the MOGA-ii operators. When an individual, In_i, is subject to directional crossover it will create a new individual, In_{i+1}, with two other same generation individuals, In_{i+2} *and* In_{i+3}, by moving in a randomly weighted direction. These two individuals, In_{i+2} *and* In_{i+3}, are the best fitness individuals from the two pools, which were created by random walks from the initial individual, In_i. The research shows that directional crossover can achieve better optimization results than the classical crossover [24].

2.2 Multi-Objective Simulated Annealing (MOSA). MOSA is a randomized search algorithm for approximating the global optimum of multiple objective functions [25]. The MOSA algorithm mimics the annealing process at which an optimization routine can randomly move along a direction with a perturbation length to reach a better optimal solution. If one perturbation solution dominant its original solution, then it will become the next staring point. Otherwise, a probability calculation based on the difference of objective functions' value between two solutions ΔE_i is used to determine if an inferior solution will be accepted. The probability of acceptance for inferior solutions id generally decreased with iterations. This approach often allows the algorithm to escape local minima. With multiple solutions being simulated in parallel, a suitable minimum for engineering purposes can often be identified.

The MOGA-II algorithm has been used in many engineering topics to determine the optimal solutions. For example, Poles et al. [26] applied MOGA-II to optimize the shape of automotive cooling ducts; the results minimized the inlet and the outlet pressure

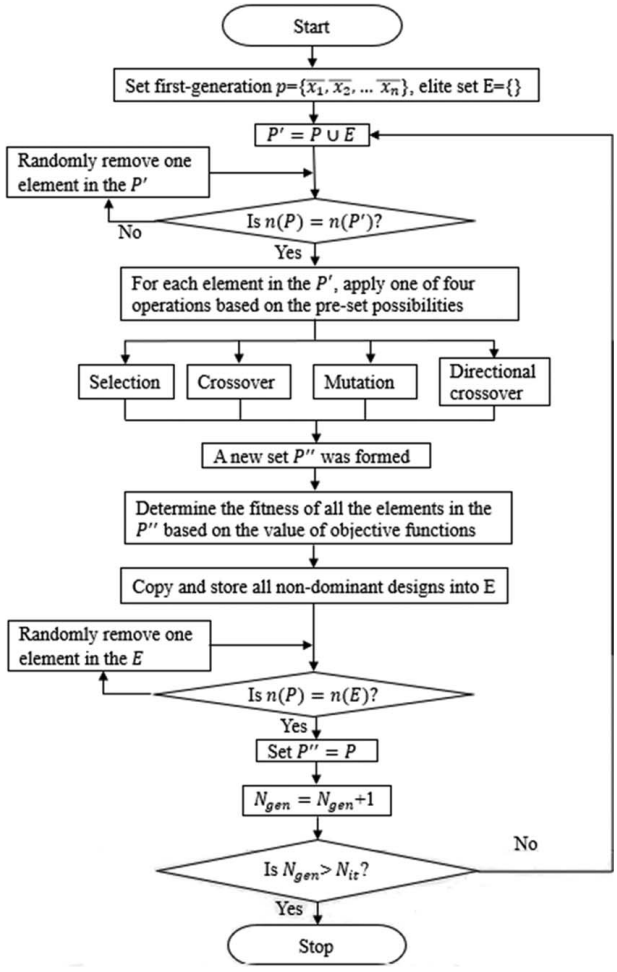

Fig. 3 The flow chart of the MOGA-II algorithm

drop while maximized the outlet flow velocity. Abidi et al. [27] used MOGA-II to optimize the input parameters for an electrical discharge machining process. For shape memory alloy machining a better material removal rate was reached with good surface finish. Mohammed et al. [28] explored MOGA-II to achieve an optimized surface roughness and material removal rate for micro-milled alumina ceramic for laser beam intensity, frequency, and pulse overlap. Alkhalefah [29] investigated parameter selection using MOGA-II for a rotary ultrasonic drilling process to achieve a combination of high material removal rate, enhanced surface finishing, and dimensional accuracy in Alumina ceramic drilling. Costa et al. [30] used MOGA-II to minimize the error between the computed model's results from a thermos-chemical equilibrium model and experimentally measured data. Finally, Ali et al. [31] optimized the fabrication conditions of polyamide thin film composite membranes with MOGA-II.

On the other hand, MOSA was applied in various research as well. Sekkal et al. [32] used MOSA to optimize the processing time and resource usage for the parallel machine scheduling problem under machine deterioration constraints. The additive manufacturing optimization problem was studied by Cao et al. [33] with MOSA a components' envelop volume and connective lines length. Turgay [34] optimized a facility layout costs and location simultaneously subject to unequal area constraints. Zidi et al. [35] utilized MOSA to achieve optimized route duration and service quality in the Dial a Ride Problem (multiple users require pickup and delivery between origins and destinations). Zaretalab [36] applied MOSA to solve the redundancy allocation problem; compared to other algorithms, better quality solutions were achieved using a memory matrix to reinforce the neighborhood structure. Lastly, Varadharajan et al [37]. minimized the mask span and total flowtime of jobs for the permutation flowshop scheduling using MOSA.

3 Tradespace Analysis

The tradespace analysis is a visual process that enables design engineers to recognize capabilities, gaps, and potential tradeoffs that facilitate the meeting of system performance objectives [38]. Mechanical systems are considered to be individual systems with their own unique architectures, and it is acknowledged that they should be assessed through tradespace studies [39,40]. Models are developed to simulate the attributes of a product based on its user's preferences and further guide the design choice. These choices are then varied systematically to produce tradespace representation. The concept of trade space refers to a range of multidimensional outputs or outcomes of interest resulting from a particular process or set of choices that cannot all be optimized simultaneously [41].

Tradespace is the space of possible design options with a given set of design variables viewed in the performance objective space. Simply put, in tradespace analysis, performance capabilities are visualized. The attributes define the system completely, which means by naming their values, people can understand how well the system reaches its overall objectives. These attributes are then aggregated into a single utility function, u_{tot}. The utility function, is a dimensionless variable that measures relative gratification by allocating the resources of an attribute. The total utility function allows the comparison of different system practicality by assigning weighting factors to every attribute. The rationale of this step is that if there is a conflict between two attributes, the designer will prioritize better performance in the more significant (higher weighting factors) attributes and make concessions on the less important (lower weighting factors) ones, thus enables the attainment of optimal design [42].

Finally, a cost model will be applied to provide a metric to compare the estimated expense for each design. These actions enable a utility-cost plot to be created to help find the highest utility for a fixed cost [43]. Similar to the MOO, the optimal design Pareto Frontier can be identified through design variable variation. Utility variables usually range from zero (minimal acceptable) to one (most desirable). Consequently, a size rule was applied to calculate the proposed system attribute. The system designs were then evaluated in consideration of the utility magnitudes to understand which design best satisfies the needs.

Designing mechanical engineering systems poses a major challenge in the early stage of concept exploration, as most engineering resources are dedicated to this phase. Therefore, critical decisions made during this phase must result in designs that provide value over the operational lifespan of the system [44]. Tradespace analysis can aid in making well-informed decisions when choosing from different designs to identify the most cost-effective solution that satisfies customer requirements. Additionally, they can facilitate the comparison and contrast of technical solutions for systems [39,44].

4 Case Study

The classical E. Howard Model 00 street clock movement from 1905 features an external weight driven gear train, escapement, and large pendulum. A mathematical model will be developed followed by experimental validation and optimization of the pendulum subsystem.

4.1 Mathematic Model. The pendulum clock with escapement provides an opportunity to derive a nonlinear dynamic system model. The hanging mass, M, acts on the winding drum of radius R_A to provide a torque $T_w = MgR_A$ that drives the movement. The gear train features five shafts or arbors, shown in Fig. 1, that significantly reduces the torque that acts on the escapement. For this clock, the train ratio, R_t, can be expressed as

$$R_t = \left(\frac{N_{B1}}{N_{A1}}\right)\left(\frac{N_{c1}}{N_{B2}}\right)\left(\frac{N_{D1}}{Nc_2}\right)\left(\frac{N_{E1}}{N_{D2}}\right) \tag{2}$$

where N denotes the number of gear teeth of the respective wheels. The torque acting on the escape wheel, T_e, becomes $T_e = 1/R_t T_w$.

The escapement provides energy to the pendulum to overcome the losses due to friction and aerodynamic forces. The escapement model was developed based on the following four assumptions:

A1. The escapement engages and disengages with the pendulum at the pendulum swing angle of $\pm\theta_e$ which is a specification for the target clock movement.
A2. The impulsive torque accelerates the pendulum to maintain oscillatory motion.
A3. The angular motion of the pendulum, θ, is symmetric.
A4. The system maybe considered stable in a dynamic sense when the angular amplitude of the pendulum's oscillation, θ, ends between $0.7\theta_e < \theta < 1.5\theta_e$.

The torque, T_A, applied by the escapement anchor to the pendulum crutch becomes

$$T_A = S_1 S_2 T_e \tag{3}$$

where S_1 and S_2 are relational digital variables that control the impulse sign based on the pendulum's angle such as

$$S_1 = \begin{cases} 1; & if\ \dot{\theta} > 0 \\ 0; & if\ \dot{\theta} = 0 \\ -1; & if\ \dot{\theta} < 0 \end{cases} \qquad S_2 = \begin{cases} 1; & if\ -\theta_e \le \theta \le \theta_e \\ 0; & otherwise \end{cases} \tag{4}$$

In this manner, the pendulum swings back and forth at a fixed period with regular impulses.

The dynamic model for the pendulum oscillation angle, θ, becomes

$$J\ddot{\theta} + B\dot{\theta} + mgLsin\theta + LF_{ai} = T_A \tag{5}$$

where $J = mL^2$ is the pendulum's moment of inertia which assumes a point mass, and B is the damping coefficient. The impulsive torque, T_A, arises every half-period due to the escape wheel and crutch drive torque. An aerodynamic drag force, F_{ai}, primarily acts on the pendulum bob to dissipate energy as it swings through the air. This force requires the drag coefficient, C_D, the surface area of the bob (and rod) acted on by the air, A, the air density, ρ_{ai}, and the translational velocity of the bob, $L\dot{\theta}$, to calculate as

$$F_{ai} = \frac{1}{2} C_D A \rho_{ai} (L\dot{\theta})^2 \tag{6}$$

The design of the pendulum system, refer to Fig. 1(*a*), was explored given its importance for clock precision. For this subsystem, the total pendulum mass, m, depends on the radius of the bob, R, the thickness of the bob, h, the rod length, L, and the rod radius, r, so that

$$m = (\pi R^2)h\rho_i + (\pi r^2)L\rho_w \tag{7}$$

where ρ_i and ρ_w are the density of the cast iron and the wood, respectively. The minimum, m_L, and maximum, m_u, pendulum mass values to maintain the system motion are define a priori given the design space operating limitations.

4.2 Experimental Validation of Mathematical Model. To validate the tower clock mathematical model, the E. Howard clock movement was experimentally investigated. Three cube-shaped high flux magnets were attached to the escape wheel pivot, crutch pivot, and pendulum using epoxy putty and a drop of adhesive. A high resolution magnetic field angular position sensor (Honeywell APS00B) with a pair of linear amplifiers (Analog Device AD623) was placed on a stick opposite each magnet as shown in Fig. 4. These magnetic signals were converted to digital signals and supplied to the National Instrument ELVIS™ data acquisition system. The host laptop procured the data files using LabView™ and Matlab™. During the experimental testing, the crutch was also removed and the pendulum was released from an angular position of 2.12 deg. The time constant, τ, represents the duration for the system's response to decay to zero if the initial decay rate had continued. Due to the progressive change in the decay rate, the actual response will have decreased in value to approximately 36.8% of its original value within this time. In this research, τ, was measured by determining the elapsed time for the initial amplitude to drop by 63.2% or 0.632*2.12 deg = 1.34 deg. The time constant for this E. Howard tower clock movement was experimentally determined to be τ = 5599 s. A portion of the pendulum's angle versus time is shown in Fig. 5 which offers the time constant free response. The operation of the escapement was also recorded and used to validate the mathematical model. Further, the various system parameters were carefully measured using a caliper and other laboratory tools. The results show for experiential measured and simulated results both pendulum period is 2.00 s. In addition, the simulated Q = 8784 corresponds to a 0.04% error from the actual clock where Q = 8780.

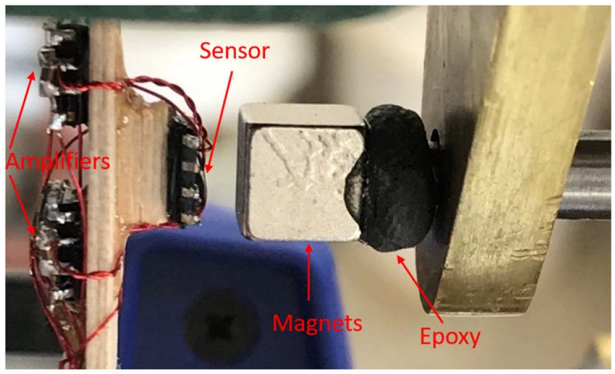

Fig. 4 E. Howard tower clock experimental testing—Magnet, sensor, and amplifier to measure the angular motion.

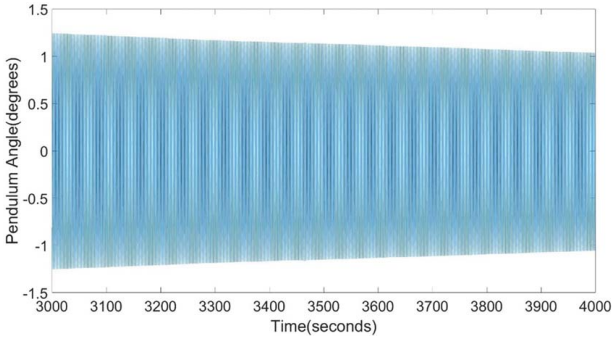

Fig. 5 Free angular response of pendulum (i.e., crutch removed) to evaluate the Quality Factor.

Table 1 Summary of model and optimization parameters

Symbol	Value	Units	Symbol	Value	Units	Symbol	Value	Units
A	0.032	m^2	N_{A1}	90	teeth	T_{des}	2.0	s
a_1	−0.035	—	N_{B1}	18	teeth	T_i	0.1	—
a_2	$4*10^{-5}$	—	N_{B2}	80	teeth	T_o	2.0	s
a_3	−5	—	N_{c1}	18	teeth	T_{des}	2.0	s
B	0.0036	N/rad/s	Nc_2	96	teeth	$x_{1,L}$	0.9	m
b_1	1.175	—	N_{D1}	12	teeth	$x_{1,o}$	0.994	m
b_2	0.125	—	N_{D2}	90	teeth	$x_{1,U}$	1.1	m
b_3	1	—	N_{E1}	12	teeth	$x_{2,L}$	0.06	m
C_D	1.6	—	N_{hot}	25	—	$x_{2,o}$	0.0825	m
C_{ir}	10.68	€/kg	N_{in}	50	—	$x_{2,U}$	0.12	m
C_o	14.24	€/m	N_{it}	50	—	$x_{3,L}$	0.04	m
g	9.81	m/s^2	N_{MO}	50	—	$x_{3,o}$	0.06	m
l_{min}	0.05	—	N_{tot}	50	—	$x_{3,U}$	0.08	m
M	13.6	kg	Q_o	8783		ρ_{ai}	1.225	kg/m^3
m_L	5	kg	R_A	0.0762	m	ρ_i	7, 800	kg/m^3
m_o	10.316	kg	R_t	1333.33		ρ_w	800	kg/m^3
m_U	25	kg	r	0.011	m	θ_e	0.02	rad

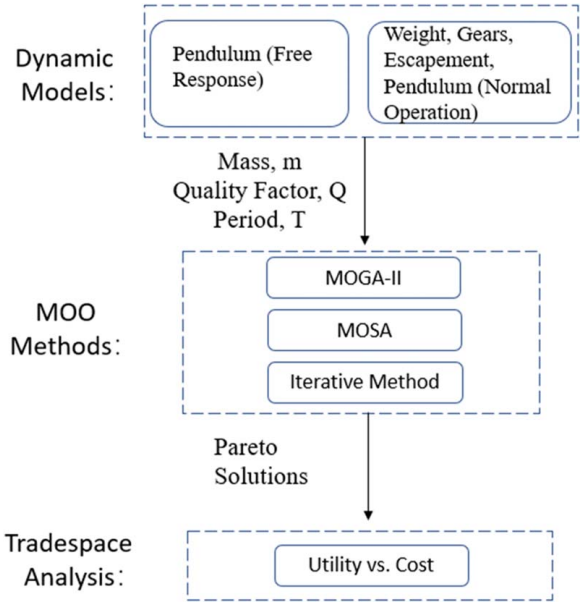

Fig. 6 The simulation and optimization process

4.3 Optimization Problem. The optimization problem was explored using MOO with MOGA-II and MOSA algorithms. The mechanical clock's overall accuracy was investigated with the design of the pendulum system's mass, Quality Factor, and period. In a pendulum system, a higher Q value tends to be more accurate due to the lower rate of energy loss. For an oscillatory system, the quality factor can be calculated as [10]

$$Q = \pi f_0 \tau \tag{8}$$

where f_0 is the system's natural frequency, and τ is the exponential time constant. For a small pendulum swing, the period, $T = 1/f_0$, can be expressed as

$$T = 2\pi\sqrt{L/g} \tag{9}$$

so that Eq. (12) becomes

$$Q = \frac{\tau}{2}\sqrt{\frac{g}{L}} \tag{10}$$

Table 2 Summary of MOO methods results

No.	Method	Total Solutions	Feasible Solutions	Pareto Solutions
1	MOSA	2500	2469	1149
2	MOGA-II	2500	2467	1162
3	Random soultion method	2500	2410	1105

Three clock parameters, $x_1 = L$, $x_2 = R$, and $x_3 = h$, were selected as the design variables. The optimization problem may be stated as

$$\min(f_1(x): \pi x_2^2 x_3 \rho_i + \pi r^2 x_1 \rho_w) \tag{11a}$$

$$\min(f_2(x) = -Q) \tag{11b}$$

$$\min(f_3(x) = |T - T_{des}|) \tag{11c}$$

Subject to:

$$x_{i,L} \le x_i \le x_{i,H} \tag{11d}$$

For this study, the system and optimization parameters are listed in Table 1. The other MOGA-ii and MOSA parameters that have not been included in Table 1 were set at default values. Overall, 2500 solutions were created during the MOGA-ii and MOSA optimization process. For comparison, the random solution method also generated 2500 solutions between the upper and lower limit of design variables.

The governing equations and MOO were coded in MATLAB™ and a two steps process followed. First, the pendulum was released from a vertical angle of $\theta = 2.0$ deg (0.035 rads), allowing the system to experience free oscillation. The time constant, τ, was calculated by determining the elapsed time for the initial amplitude to drop by 63.2% or 0.632*2 deg = 1.264 deg. The variables m and Q were computed for every solution. Second, the pendulum received an impulsive torque, T_A, (i.e., engage and disengage with the pendulum rod every half period) due to the clock escapement. The period was calculated after the clock was operating for 600 s. Afterwards, the results were supplied to the modeFRONTIER® tool where the multi-objective optimization process was performed. The simulation and optimization process has been displayed in Fig. 6.

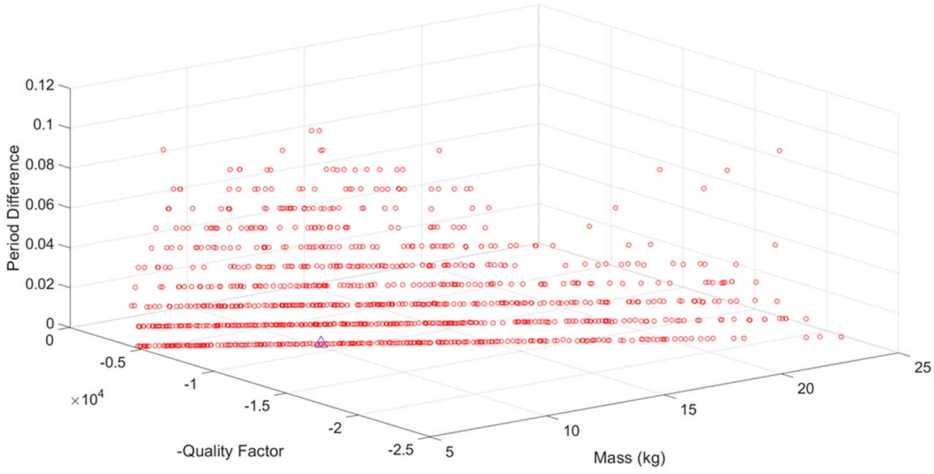

Fig. 7 MOGA-II Pareto solutions (o) and original design (Δ) for the tower clock

Table 3 Proposed weighting factors for design aspects A-C in mechanical clock study

Design aspect	Description	Weighting		
		w_m	w_Q	$w_{\Delta T}$
A	Smaller mass	0.6	0.3	0.1
B	Higher accuracy	0.3	0.6	0.1
C	Nominal design	0.33	0.33	0.33

4.4 Optimization Results. All of three MOO methods are supposed to generate Pareto solutions, however, the number of feasible and Pareto solutions is an indicator of the effectiveness of the MOO method. Three groups of 2500 solutions were collected and further analyzed in MATLAB™ and modeFRONTIER® to obtain the feasible and Pareto solutions. The high level results are summarized in Table 2. It may be observed that the MOSA, MOGA-II and random solution method all reach the real Pareto-frontier and preserve the computations in the feasible region.

To offer insight into the design process, the MOGA-II method (o) Pareto solutions and the original E. Howard clock's design (Δ) are shown in Fig. 7. The optimal design was dominated by the Pareto solution, $\bar{x} = [1.002, 0.089, 0.051]$, which corresponds to a mass of 10.258 kg, a quality factor of 8843, and a period of 2.0 s. In the study, the period difference is evaluated at steady-state operation which occurs near the end of each numerical simulation run. The original 1905 design was $\bar{x}_o = [0.994, 0.0825, 0.06]$ as measured directly from the E. Howard clock. In a comparison of the two solutions, the optimal design values differ by $\Delta\bar{x} = [+0.8\%, +7.9\%, -15\%]$. In terms of the objective functions, the differences are a 0.56% reduction in the mass, a 0.7% increment in the Quality Factor, and a value of similar period. Sand casting was the common method for manufacturing cast iron pendulum bobs circa 1900. Considering that the current manufacturing tolerance for sand casting is approximately 0.5%, the original 1905 design can be improved further.

4.5 Tradespace Analysis. Tradespace analysis enables the investigation of the design with the highest utility at a fixed cost among the MOO-based Pareto solution. The pendulum subsystem features were translated into a single linear utility function, u_{tot}, given as

$$u_{tot} = w_m v_m + w_Q v_Q + w_{\Delta T} v_{\Delta T} \tag{12}$$

where w_i is the weighting factor that allows emphasis of different aspects as shown in Table 3. w_i are assigned base on our assumption for different design aspects.

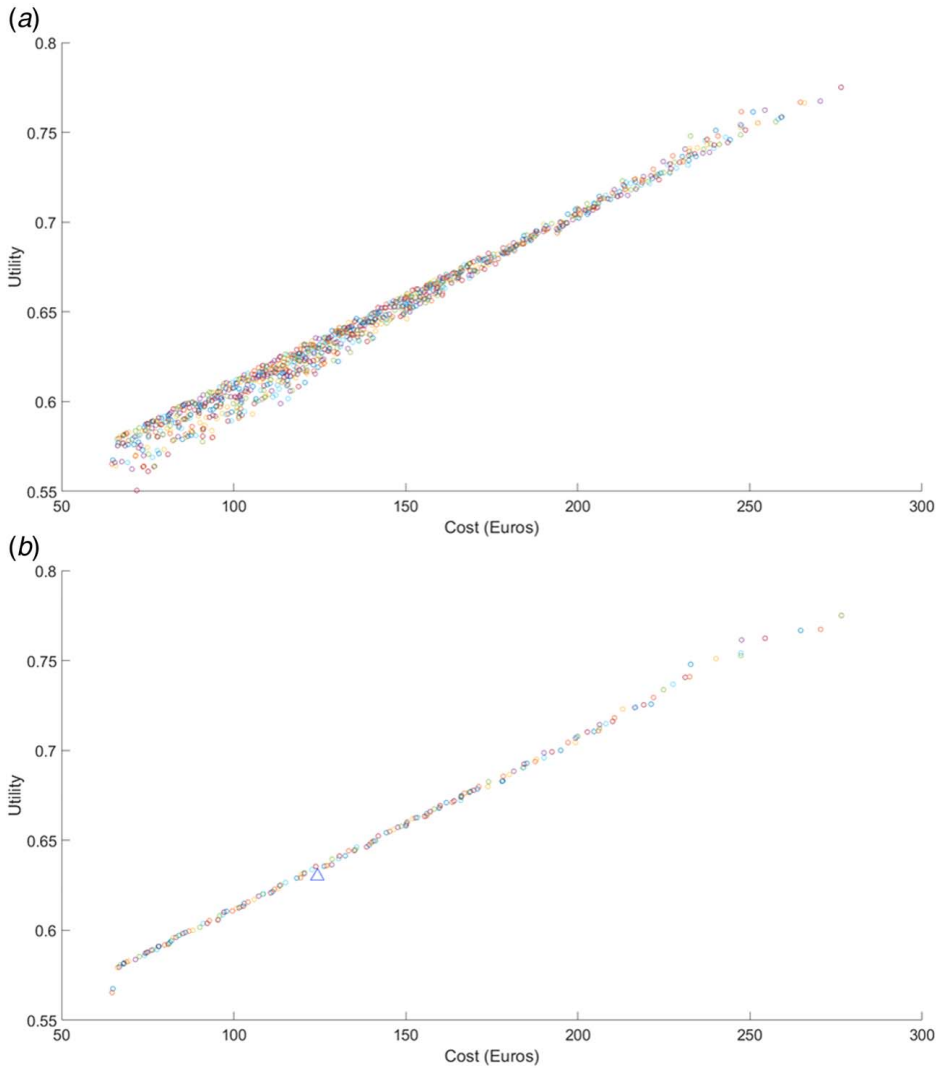

Fig. 8 Optimization study results—(*a*) Tradespace analysis result for Design Aspect B, and (*b*) Selected optimal designs with original E. Howard design shown in the Δ symbol.

The formulation of the weighted objective function, representing the value function of the system in this case, allows for the identification of the Pareto solutions for this problem as the underlying value functions are linear functions supporting a convex feasible solution space in the objective space. For nonlinear formulations where convexity cannot be guaranteed a goal oriented approach would be more appropriate.

The clock pendulum financial cost was estimated based on the mass of the materials used in the design excluding manufacturing. A typical pendulum was made of cast iron, ρ_i, for the bob; and wood, ρ_w, for the rod. For the bob and the rod shape materials, the prices of the cast iron C_{ir}, and the oak, C_o, were assigned per the current market values. The minimum and maximum values of the MOO Pareto solutions are listed in Table 1. A linear utility relationship has been assumed between the mass, the Quality factor, and the period difference so that

$$v_m = a_1 m + b_1 \tag{13a}$$

$$v_Q = a_2 Q + b_2 \tag{13b}$$

$$v_p = a_3 |T - 2| + b_3 \tag{13c}$$

To explore the utility function, one of the tower clock design aspects will be presented with comparisons to the original design. Figure 8(*a*) displays the tradespace analysis for Design Aspect B (Higher accuracy) with utility versus cost; each point represents an optimal solution obtained by the MOGA-II method. The Pareto Designs of 8(a) are extracted In Fig. 8(*b*), a clear Pareto Frontier, which indicates desirable designs, can be observed. The original design of the pendulum clock is also shown on this plot with a Δ symbol. It can be observed that the original design is slightly off the Pareto Frontier which means that the total utility of original design could be enhanced further without a price increase.

5 Conclusion

The working principle of a classical pendulum mechanical clock and three system parameter design, the MOO, and the tradespace analysis method has been reviewed. A lumped parameter mathematical model of the pendulum clock has been developed. To achieve optimum pendulum design, its mass, quality factor, and clock accuracy have been explained with two MOO methods. The MOGA-II/MOSA algorithm is efficient in finding the Pareto optimal solutions compared to a random solution method. The MOO results also demonstrate that a better quality factor lightweight design can be achieved without changing the original period. The tradespace result further expands the possible design option for the pendulum clock.

Conflict of Interest

There are no conflicts of interest. This article does not include research in which human participants were involved. Informed consent not applicable. This article does not include any research in which animal participants were involved.

Data Availability Statement

The authors attest that all data for this study are included in the paper.

Nomenclature

A = Effective pendulum area (m^2)
a_i/b_i = Fit Parameters in tradespace analysis
B = Damping coefficient of pendulum (N/rad/s)
C_D = Drag coefficient
C_{ir} = Bob shape iron price for (€/kg)
C_o = Pendulum shape oak price (€/m)
E = Elite set in MOGA-II
F_{ai} = Air resistance (N)
f_0 = Frequency of pendulum (Hz)
$f_i(\bar{x})$ = Objective functions for MOO
g = Gravity (m/s^2)
$g_j(\bar{x})$ = Equality constraints for optimization
$h_k(\bar{x})$ = Inequality constraints for optimization
h = Thickness of the bob (m)
In_i = Individual in MOGA-II
J = Pendulum moment of inertial ($Kg{\cdot}m^2$)
L = Length of pendulum rod (m)
M = Hanging weight mass (kg)
m = Pendulum rod and bob mass (kg)
m_L = Lower limit for pendulum mass keeps the system stable
m_u = Upper limit for pendulum mass keeps the system stable
N_{ij} = Number of teeth as j^{th} gear on i^{th} arbor
N_{in} = Number of population in first generation for MOGA-II
N_{it} = Iteration number stop criteria for MOGA-II
P/P′/P″ = A Generation in MOGA-II
Q = Quality factor
R = Bob radius (m)
R_A = Radius of winding drum (m)
R_t = Train ratio
r = Pendulum rod radius (m)
s_i = Relational digital variables
T = Period (s)
T_A = Escapement anchor toque (Nm)
T_{des} = Pendulum desire period (s)
T_e = Escape wheel torque (Nm)
T_w = Hanging weight torque (Nm)
u_{tot} = Total utility
v_m = Single attribute utility for mass
$v_{\Delta t}$ = Single attribute utility for period difference
v_Q = Single attribute utility for quality factor
w_m = Utility weighing for mass
$w_{\Delta t}$ = Utility weighing for period difference
w_Q = Utility weighing for quality factor
x_i = Design variables
x_L = Lower limit for design variables
x_H = Upper limit for design variables
$x_{p,i}$ = Design variables of Pareto solution
$\bar{x}$ = Design variable vector
$\bar{x}_p$ = Pareto solution design variable vector
θ = Pendulum angular (rad)
θ_e = Amplitude of pendulum swing (rad)
τ = Time constant (s)
ρ_{ai} = Density of air (kg/m^3)
ρ_i = Iron density (kg/m^3)
ρ_w = Wood density (kg/m^3)
ΔE_i = Energy between two MOSA solutions (J)

Subscript

o = E. Howard clock initial parameters

References

[1] Wagner, J., Knaub, H. K., Volk, E., and Jagarwal, A., 2010, "Modeling and Analysis of a Weight Driven Mechanical Tower Clock," American Control Conference, Baltimore, MD, pp. 634–639.
[2] Penman, L., 2002, *Practical Clock Escapements*, Mayfield Books, Vitoria, Spain.
[3] Denny, M., 2002, "The Pendulum Clock: A Venerable Dynamical System," Eur. J. Phys., **23**(4), pp. 449–458.
[4] Wagner, J., Huey, C., and Knaub, K., 2008, "Clock Mechanism Fundamentals for Education: Modeling and Analysis," ASME Dynamics Systems and Control Conference, Ann Arbor, MI, pp. 1-8.
[5] Matthys, R., 2004, *Accurate Clock Pendulums*, Oxford University, Oxford, Great British.
[6] Smith, N., 2015, "A Technique for Continuous Measurement of the Quality Factor of Mechanical Oscillators," Rev. Sci. Instrum., **86**(5), p. 053907.

[7] Feinstein, G., 2006, "Impulsing the Pendulum: Escapement Error," NAWCC Horol. Sci., **161**(3), pp. 569–575.
[8] Nawrodt, R., Zimmer, A., Koettig, T., Schwarz, C., Heinert, D., Hudl, M., Neubert, R., et al., 2008, "High Mechanical Q-Factor Measurements on Silicon Bulk Samples," J. Phys. Conf. Ser., **122**, p. 012008.
[9] Burke, E. K., and Kendell, G., 2014, *Search Methodologies: Introductory Tutorials in Optimization and Decision Support Techniques*, Springer, New York, Chap. 15.
[10] Ngatchou, P., Zarei, A., and El-Sharkawi, M. A., 2005, "Pareto Multi Objective Optimization," Proceeding of the 13th International Conference, Arlington, VA, pp. 84-91.
[11] Konak, A., Coit, D. W., and Smith, A. E., 2006, "Multi-Objective Optimization Using Genetic Algorithms: A Tutorial," Reliab. Eng. Syst. Saf., **91**(9), pp. 992–1007.
[12] Browne, D. C., Fullmer, D. D., Slusser, D. S., Stone, R., and Terrell, G. R., 2016, "Improving DoD Acquisition with Set-Based Design," 19th Annual Systems Engineering Conference, Springfield, VA, Oct. 27.
[13] McGowan, D., and Lichty, N., 2019, "Framework for Developing Model-Based Buy Packages," 2019 Global Product Data Interoperability Summit, Phoenix, AZ, Sept. 16–19.
[14] Parnell, G., Madni, A., and Bordley, R., 2017, "A Conceptual Framework and Mathematical Foundation for Trade-off Analysis," *Trade-Off Analytics: Creating and Exploring the System Tradespace*, G. Parnell, ed., John Wiley and Sons, Inc., Hoboken, NJ.
[15] Daniels, J., Wagner, J., Turner, C., Gorsich, D., Rizzo, D., Hartman, G., Agusti, R., Skowronska, A., Castanier, M., and Rapp, S., 2022, "Tradespace Practices in Organizations: A Case Study," Proceedings of the 2022 ASME International Design Engineering Technical Conferences Computers and Information in Engineering Conference, American Society of Mechanical Engineering, St. Louis, MO, Aug. 15–17.
[16] Daniels, J., Masoudi, N., Wagner, J., Turner, C., Hartman, G., Rizzo, D., Gorsich, D., Skowronska, A., and Agusti, R., 2022, "Designing the Design Space: Evaluating Best Practices in Tradespace Exploration, Analysis and Decision-Making," Proceedings of the 2022 SAE WCX, Detroit, MI, April.
[17] Specking, E., Parnell, G., Pohl, E., and Buchanan, R., 2018, "Early Design Space Exploration with Model-Based System Engineering and Set-Based Design," Systems, **6**(4), p. 45.
[18] Dillon-Merrill, R. L., Parnell, G. S., Buckshaw, D. L., Hensley, W. R., Jr., and Caswell, D. J., 2008, "Avoiding Common Pitfalls in Decision Support Frameworks for Department of Defense Analyses," Milit. Oper. Res., **3**(2), pp. 19–31. Available, from https://www.jstor.org/stable/43920755
[19] Simpson, T. W., Miller, S., Tibor, E. B., Yukish, M. A., Stump, G., Kannan, H., Mesmer, B., Winer, E. H., and Bloebaum, C. L., 2017, "Adding Value to Trade Space Exploration When Designing Complex Engineered Systems," Syst. Eng., **20**(2), pp. 131–146.
[20] Witus, G., and Bryzik, W., 2015, "Progress Toward a DoD Ground Vehicle Tradespace and Affordability Analysis Framework," Procedia Comp. Sci., **44**, pp. 537–546.
[21] Xiong, Y., Duong, P. L. T., Wang, D., Park, S., Ge, Q., Raghavan, N., and Rosen, D. W., 2019, "Data-Driven Design Space Exploration and Exploitation for Design for Additive Manufacturing," ASME J. Mech. Des., **141**(10), p. 101101.
[22] Geletu, A. 2007 "Solving Optimization Problems using the Matlab Optimization Toolbox—A Tutorial," TU-Ilmenau, Fakultät für Mathematik und Naturwissenschaften.
[23] Whiley, D., 1994, "A Genetic Algorithm Tutorial," Stat. Comput., **4**(2), pp. 65–85.
[24] Poles, S., 2003, "MOGA-II: An Improved Multi-Objective Genetic Algorithm," Technical Report No. 2003-006, Esteco, Trieste, Italy.
[25] Amine, K., 2019, "Multi-Objective Simulated Annealing: Principles and Algorithm Variants," Adv. Oper. Res., **2019**, pp. 1–13.
[26] Poles, S., Geremia, P., Campos, F., Weston, S., and Islam, M., 2007, "MOGA-II for an Automotive Cooling Duct Optimization on Distributed Resources," International Conference on Evolutionary Multi-Criterion Optimization, Springer, Berlin/Heidelberg, pp. 633–644.
[27] Abidi, M. H., Al-Ahmari, A. M., Umer, U., and Rasheed, M. S., 2018, "Multi-Objective Optimization of Micro-Electrical Discharge Machining of Nickel-Titanium-Based Shape Memory Alloy Using MOGA-II," Measurement, **125**, pp. 336–349.
[28] Mohammed, M. K., Umer, U., and Al-Ahmari, 2017, "A Optimization of Laser Micro Milling of Alumina Ceramic Using Radial Basis Functions and MOGA-II," Int. J. Adv. Manuf. Technol., **91**(5–8), pp. 2017–2029.
[29] Alkhalefah, H., 2020, "Precise Drilling of Holes in Alumina Ceramic (Al_2O_3) by Rotary Ultrasonic Drilling and its Parameter Optimization Using MOGA-II," Materials, **13**(5), pp. 1059–1077.
[30] Costa, M., Villetta, M. L., and Massarotti, N., 2015, "Optimal Tuning of a Thermo-Chemical Equilibrium Model for Downdraft Biomass Gasifiers," Chem. Eng. Trans., **43**(5), pp. 439–444.
[31] Ali, F. A. A., Alam, J., Shukla, A. K., Alhoshan, M., Abdo, B. M. A., and Al-Masry, W. A., 2020, "A Novel Approach to Optimize the Fabrication Conditions of Thin Film Composite RO Membranes Using Multi-Objective Genetic Algorithm II," Polymers, **12**(2), pp. 494–510.
[32] Sekkal, N., and Belkaid, F., 2020, "A Multi-Objective Simulated Annealing to Solve an Identical Parallel Machine Scheduling Problem With Deterioration Effect and Resources Consumption Constraints," J. Combin. Optim., **40**(3), pp. 660–696.
[33] Cao, P., Fan, Z., Gao, R. X., and Tang, J., 2019, "Harnessing Multi-Objective Simulated Annealing Toward Configuration," Robot. Comput. Integr. Manuf., **57**(1), pp. 29–45.
[34] Turgay, S., 2018, "Multi Objective Simulated Annealing Approach for Facility Layout Design," Int. J. Math. Eng. Manag. Sci., **3**(4), pp. 365–380.
[35] Zidi, I., Zidi, K., Mesghouni, K., and Ghedira, K., 2011, "A Multi-Agent System Based on the Multi-Objective Simulated Annealing Algorithm for the Static Dial a Ride Problem," Proceedings of the 18th World Congress The International Federation of Automatic Control, Milano, Italy, pp. 2172–2177.
[36] Zaretalab, A., Hajipour, V., Sharifi, M., and Shahriari, M. R., 2015, "A Knowledge-Based Archive Multi-Objective Simulated Annealing Algorithm to Optimize Series–Parallel System with Choice of Redundancy Strategies," Comput. Ind. Eng., **80**, pp. 33–44.
[37] Varadharajan, T. K., and Rajendran, C., 2005, "A Multi-Objective Simulated Annealing Algorithm for Scheduling in Flowshops to Minimize the Makespan and Total Flowtime of Jobs," Eur. J. Oper. Res., **167**(3), pp. 772–795.
[38] Spero, E., Avera, M. P., Valdez, P. E., and Goerger, S. R., 2014, "Tradespace Exploration for the Engineering of Resilient Systems," Procedia Comput. Sci., **28**, pp. 591–600.
[39] Blackburn, T., Mazzuchi, T., and Sarkani, S., 2012, "Using a TRIZ Framework for Systems Engineering Trade Studies," Systems Engineering, **15**(3), pp. 355–367.
[40] Blanchard, B., and Fabrycky, W., 2006, *Systems Engineering and Analysis*, Pearson Prentice Hall, Upper Saddle River, NJ.
[41] Bond, C., Mayer, L., McMahan, M., Kallimani, J., and Sanchez, R., 2015, "Developing a Methodology for Risk-Informed Trade-Space Analysis in Acquisition," U.S. Army, Available from http://www.rand.org/t/RR701
[42] Hari, A., Kasser, J., and Weiss, M., 2007, "How Lessons Learned From Using QFD led to the Evolution of a Process for Creating Quality Requirements for Complex Systems," Syst. Eng., **10**(1), pp. 45–63.
[43] Ross, A. M., and Hasting, D. E., 2005, "The Tradespace Exploration Paradigm," INCOSE International Symposium, vol. 15, No.1, pp. 1706–1718.
[44] Chattopadhyay, D., Ross, A., and Rhodes, D., 2009, "A Practical Method for Tradespace Exploration of Systems of Systems," AIAA SPACE 2009 Conference, Pasadena, CA, Sept. 14–17.